Temperature dependence of the gaps of high-temperature superconductors in the Fermi-arc region

S. Hüfner[1,2] and F. Müller[1]
[1]*Department of Experimental Physics, Saarland University, 66123 Saarbrücken, Germany*
[2]*Department of Physics and Astronomy, University of British Columbia, Vancouver, British Columbia, V6T 1Z1, Canada*
(Received 14 January 2008; revised manuscript received 22 March 2008; published 23 July 2008)

It is shown how in a high-temperature superconductor, the length of the Fermi arc can be obtained from the doping dependence of the pseudogap and the superconducting gap. In the momentum region spanned by the Fermi arc, the pseudogap temperature dependence follows that of the superconducting gap. The close interconnection of the two gaps suggests that they are both an essential part of the high-temperature superconductivity.

DOI: 10.1103/PhysRevB.78.014521 PACS number(s): 74.20.−z, 74.25.Jb, 74.25.Bt, 74.25.Dw

I. INTRODUCTION

Since their discovery,[1] high-temperature superconductors (HTSC) have been actively investigated. Among the most puzzling properties exhibited by them are two gaps, the so-called pseudogap,[2,3] which, with respect to temperature, extends well into the nonsuperconducting regime and the superconducting gap, which can be considered as the order parameter because it follows T_c.[2,4,5] In this paper, we call the superconducting gap the excitation energy, which is often called the magnetic resonance energy.[6,7]

There are two views with respect to the two gaps observed in the HTSC.[8] One assumes that the pseudogap has nothing to do with the superconductivity but rather reflects the occurrence of competing order. The other one assumes that the pseudogap is a necessary ingredient of superconductivity.[9–12] In this paper, the second view is assumed for the following reason: The doping dependence of T_c can be calculated as the product of the (free) charge carrier density and the pseudogap energy, leading to a parabolic dependence of T_c on the doping x.[11] It will be shown that the length of the Fermi arc at T_c can be estimated by interconnecting the pseudogap and the superconducting gap. In addition, the assumption that the pseudogap states are (above T_c) the precursor states to superconductivity gives a natural coupling mechanism for the HTSC. Most of this is missing in the competing order scenario[8] and, therefore, we prefer a picture where the pseudogap is a necessary building component of the HTSC.

In this paper, we refer to the value 2Δ as the total gap and call it the pseudogap energy (E_{pg}) and the superconducting energy (E_{sc}), respectively. This choice of nomenclature is made because only the value 2Δ has been measured so far for the superconducting gap such as, e.g., by neutron or Raman scattering.[6,7] As a consequence, it seems advisable to define also the pseudogap by its full value. In many experiments such as, e.g., angle-resolved photoemission spectroscopy (ARPES),[3] only half the energy, namely Δ, is measured because this is a one-electron spectroscopy and determines the energy of the electron left behind.[3]

The pseudogap and the superconducting energies have different doping dependencies,[2,4,8] as shown in Fig. 1(a). The pseudogap energy exhibits an approximately linear doping

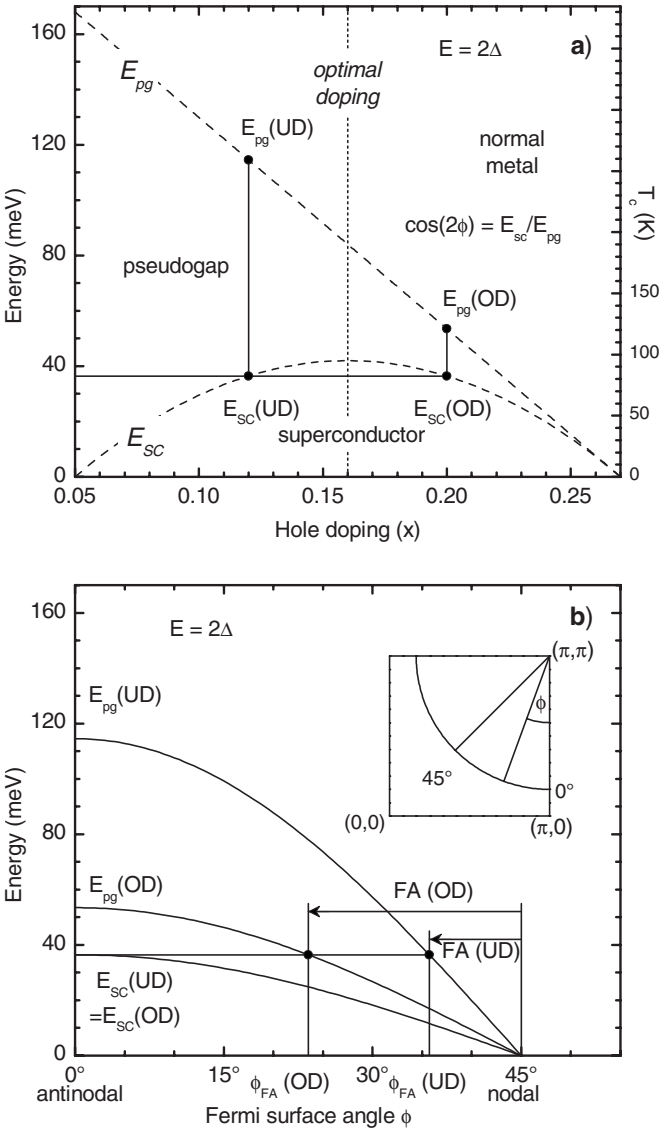

FIG. 1. (a) Phase diagram of a HTSC. The pseudogaps for an UD sample and an OD sample, with the same transition temperature T_c, are indicated, (b) The angular dependence of the superconducting and the two pseudogap energies from the top part of the figure. The Fermi-arc lengths ($45°-\phi$) are constructed for both cases.

dependence, starting with zero at about $x=0.27$ and increasing to its maximum value at $x=0.05$ [for systems with a maximum $T_c \sim 95$ K; the value $E_{pg}(x=0.05)=168$ meV is slightly larger than the one originally quoted (152 meV) due to a different fitting routine used here: Instead of a free fit to the data, as performed in Ref. 4, it was assumed that the E_{pg} line is the tangent of the E_{sc} parabola at $x=0.27$]. On the other hand, the superconducting energy (or the order parameter) has a parabolic doping dependence, going to zero at maximum and minimum doping. The two gaps are related to $E_{sc}=E_{pg}D$, with D describing the charge carrier density.[5,9–11] Both curves in Fig. 1(a) are the average of data from many different experimental techniques.

The pseudogap energy is always larger than the superconducting energy. This shows that the HTSC are not classical BCS superconductors but rather represent systems intermediate between a BCS and a Bose–Einstein (BE) condensate.[12–14] The BCS situation is a rather a unique one in that the coupling energy of two electrons to a boson is also the order parameter. In a BE system, on the other hand, there are always two energies connected with the condensate: the coupling energy of the two electrons to a boson, which can be very large compared to the second energy, and the condensation energy, which represents the order parameter. For example, in liquid He, the condensation energy is 2 K (0.2 meV) while the binding energy for the boson is 20 eV, which gives a value of 100 000 for the ratio of the coupling and condensation energies. Figure 1(a) shows that in the HTSC, the ratio of the coupling energy to the condensation energy ranges from 1 at $x=0.27$ to infinity at $x=0.05$.

One-electron spectroscopies such as ARPES or scanning tunnel microscope[3,15] (STM) probe half the pseudogap energy because they determine the break up of a pair of electrons. These techniques cannot measure (in the one-electron mode) the order parameter or the superconducting energy because, in the HTSC, the break up energy of a boson is always larger than the boson condensation energy, which determines the superconducting properties.

On the other hand, Andreev reflection[16] measures the injection of a pair of electrons into the superconducting condensate and, therefore, it measures the superconducting energy (a pair of electrons). The neutron and Raman scattering[6,7] are the reverse processes in which they measure the energy needed to remove a boson from the condensate.

From the theoretical point of view, the curves in Fig. 1(a) are well reproduced by theories[9,10] based on the original concept of the resonating valence bond theory.[17] While the general concept that explains the physics of the HTSC seems to be established, there are numerous details that still have to be worked out. In this paper, the temperature dependence of the ARPES spectra in the Fermi-arc regime will be analyzed,[18–20] showing that the pseudogap and the superconducting energies are intimately connected.

II. TEMPERATURE DEPENDENCE OF THE PSEUDOGAP AND SUPERCONDUCTING ENERGIES

The pseudogap represents incoherent pairs of electrons produced from the Zhang–Rice singulets.[21,22] With increasing temperature, their antiferromagnetic coupling is broken up and disappears[2] at the so-called pseudogap temperature T^*, which is larger than T_c. If measured at the position of its maximum near the antinodal point $(\pi/0)$ by ARPES[3] or STM[15] experiments, the magnitude of the pseudogap has only little changes if the sample goes from the superconducting into the normal conducting state because this transition is driven by the superconducting energy, which is smaller than the pseudogap energy. This near constancy of the pseudogap energy near the antinodal point in going through the superconducting temperature has given rise to the notion that in going from above T_c to below T_c, the pseudogap changes smoothly into the superconducting gap.[3,15] This statement seems to be invalid because a one-electron spectroscopy such as ARPES measures the pseudogap energy and not the two electron superconducting energy. This latter energy is measured in Raman (B_{2g} symmetry) or neutron scattering experiments.

The interpretation of the neutron data is by no means established at this point.[23,24] It is only the resonance that vanishes at T_c (or near T_c) while other parts of the spectra persist above T_c. In addition, there is a dispersion of the resonance that has to be accounted for. Then, it is not obvious how the singlet triplet excitation couples to the superconductivity. Finally, the signal is only a few percent from what is expected from the sum rule.

In a recent paper, Lee *et al.*[18] found, by ARPES experiments, a second gap in the HTSC Bi2212 near the nodal direction, which exhibits the typical BCS temperature dependence, namely, vanishing at T_c. They contrast this gap with the pseudogap observed near the antinodal direction, which does not change its magnitude in going through T_c. In their experiments, Lee *et al.*[18] worked closely to $\phi=45°$ [the definition of ϕ is indicated in Fig. 1(b)]. It is not easy to understand why the same experiment (ARPES) should measure the pseudogap near $(\pi/0)$ and the superconducting gap near $(\pi/2/\pi/2)$. In this paper, it will be shown that the ARPES always probes the pseudogap and that, however, its temperature dependence is different in different regions of the Fermi surface.

The general reasoning for the analysis of the ARPES experiment is given in Fig. 1. In Fig. 1(a), the pseudogaps E_{pg}(OD) in the overdoped and E_{pg}(UD) in the underdoped branches of the phase diagram and the corresponding $E_{sc}(UD)=E_{sc}$(OD) are indicated for one particular T_c smaller than the maximum T_c. In Fig. 1(b), the well-known anisotropy of the two pseudogap energies [E_{pg}(UD) and E_{pg}(OD)], and the superconducting energy [E_{sc}(UD) $=E_{sc}$(OD)], are shown and measured as a function of the angle ϕ (counted from the antinodal point with $\phi=0°$ to the nodal point with $\phi=45°$). The maximum values are at $\phi=0°$ (antinodal direction) and decrease to zero at $\phi=45°$ with a $\cos(2\phi)$ dependence. Figure 1(b) shows that the maximum superconducting energy E_{sc}(UD)$=E_{sc}$(OD) intersects the two different $E_{pg}(\phi)$ curves at different angles ϕ_{FA}(OD) and ϕ_{FA}(UD) that give the length of the so-called Fermi arcs (measured from 45°, thus, being $45°-\phi$) and, as verified by the experiment, the arc is longer for the OD sample than for the UD sample.[19,20]

The Fermi arcs are pieces of the Fermi surface that occur "abruptly" at T_c out of the nodal points. For $T>T_c$, the

length of the Fermi arcs is temperature dependent and they develop into a full Fermi surface at T^*. The general T/T^* dependence of the length of the Fermi arcs shows that their lengthening is a thermally activated process.[19,20]

The temperature dependence of the pseudogap energy for an angle ϕ larger than the Fermi-arc angle will follow the temperature dependence of the superconducting energy because, in this ϕ regime, the maximum superconducting energy is larger than the pseudogap energy and the former one determines the thermodynamic behavior of the system below T_c. This is in accordance with the development of the Fermi arcs in that near nodal area.

Therefore, the closing of the superconducting gap (or the disappearance of the superconducting energy) leads, in the region of the Fermi surface given by $E_{pg}(\phi) < E_{sc}(\phi=0)$, to a simultaneous closing of the (smaller) pseudogap. This region is larger in the OD sample than in the UD sample [see Fig. 1(b)].

These general considerations will now be adapted to the experiment of Lee *et al.*[18] They performed their experiment on a UD92 sample near the nodal point with relatively small pseudogap energies of 34, 28, and 20 meV. The maximum pseudogap energy for their 92 K sample is around 80 meV [from Fig. 2(b) of Ref. 18] at $\phi=0°$ (the authors give, in their study, Δ instead of 2Δ, which was used here). The superconducting energy of their system can be estimated as (46 ± 8) meV at $\phi=0°$ from Fig. 3(b) in Ref. 18.

A brief remark with respect to the numbers to be discussed is important. If one determines the low temperature ARPES gap values for the cuts C1, C2, and C3 [from Fig. 2(d) in Ref. 18], one gets 20 (point A), 34 (point B), and 28 meV (point C) (note that these are twice the numbers given by the authors due to our use of 2Δ). However, if one uses Fig. 3(a) from Ref. 18 to extract the same numbers, one finds 16 (point A), 36 (point B), and 24 meV (point C). It is emphasized that this statement is not intended as a criticism of the authors of Ref. 18, but it is made in order to give the reader an idea of the error bars of data in this field.

In order to document an example for the scatter of the numbers, Table I compares the Fermi angles that are derived from the data in Ref. 18 by different procedures. If one determines the Fermi angles for the data points A, B, and C, indicated in Fig. 2(d), one obtains $\phi=35°$, 30°, and 33°, as measured from the antinodal direction (column 2 of Table I). If one assumes a *d*-wave behavior for the gap, the experimental values [Fig. 2(d) in Ref. 18] for the gaps of 20 (point A), 34 (point B), and 28 meV (point C) lead together with a zero angle ($\phi=0°$) gap of 80 meV [Fig. 3(b) in Ref. 18] to angles of 38° (point A), 32° (point B), and 35° (point C) (last column of Table I). In contrast, for a zero angle gap of 99.3 meV [as deduced from Fig. 1(a) via the $T_c=92$ K value of the sample] the same procedure results in angles of 39° (point A), 35° (point B), and 37° (point C) (column 4 of Table I). While these kinds of inconsistencies are not unusual in the field and probably unavoidable, one has to be aware of them.

Here, the experimental data from Refs. 18–20 are compared to the results of the model given in Fig. 1, with a linear doping dependence of the pseudogap energy $E_{pg} = 168/0.22(0.27-x)$ (in meV) and a parabolic doping dependence of the superconducting energy $E_{sc}=42[1-82.64\cdot(x-0.16)^2]$ (in meV). In view of the spread in the experimental data, as indicated above, we use the values obtained from the straight lines in Fig. 1 (column 4 of Table I) in order to get a more general picture of the situation.

TABLE I. Data for UD92 sample, as given by Ref. 18 and by this work; $\phi_{\min}=27°$ taken from Fig. 3(b) of Ref. 18; $\phi_{\min}=33°$ from $\cos(2\phi_{\min})=40.7$ meV/99.3 meV as taken from Fig. 2(b); $\phi_{\min}=27°$ from $\cos(2\phi_{\min})=46$ meV/80 meV, as taken from Ref. 18;

1	2 ϕ [a] ($\phi_{\min}=27°$)	3 $E_{pg}^{\max}(\phi)$ [a]	4 ϕ [b] ($\phi_{\min}=30°$)	5 ϕ [c] ($\phi_{\min}=27°$)
A	35°	20 meV	39°	38°
B	30°	34 meV	35°	32°
C	33°	28 meV	37°	35°

[a]Values taken from Fig. 2(d) of Ref. 18.
[b]Calculated from $\cos(2\phi)=E_{pg}^{\max}(\phi)/E_{pg}(\phi=0)$, with $E_{pg}(\phi=0)=99.3$ meV for the UD92 sample from Fig. 1(a) of this work.
[c]Calculated from $\cos(2\phi)=E_{pg}^{\max}(\phi)/E_{pg}(\phi=0)$, with $E_{pg}(\phi=0)=80$ meV for the UD92 sample from Fig. 3(a) of Ref. 18.

For an analysis of the data of Lee *et al.*,[18] Fig. 1 is now redrawn with the specific parameters of their experiment, namely, a UD92 Bi2212 sample. The doping of the sample ($x=0.14$) was determined by the intersection of the $T=92$ K line with the E_{sc} parabola in the underdoped region. Taking the numbers from Fig. 2(a), this sample has a maximum pseudogap energy of about 99.3 meV and a corresponding superconducting energy of 40.7 meV [cf., full lines in Fig. 2(a)]. According to Fig. 2(b), these values result in a Fermi-arc angle of $\phi=33°$ (note that a small Fermi-arc angle gives a large Fermi-arc length).

The temperature dependent gaps were measured by Lee *et al.*[18] for the UD92 sample at $\phi=39°$ (point A), 35° (point B), and 37° (point C), if one takes the numbers from column 4 of Table I. All values are situated in the ϕ region above $\phi=33°$, where the Fermi arc occurs at $T=T_c$. Therefore, Lee *et al.*[18] have measured the temperature dependence of pseudogap energies (34, 28, and 20 meV) all smaller than the superconducting energy for the UD92 sample, which is 40.7 meV from Fig. 1(a). Thus, they see the thermodynamics governed by the superconducting energy scale and not that of the pseudogap energy scale. Their observation is not unexpected because the collapse of the pseudogap at T_c into the Fermi arc is a well documented fact[19,20] and Lee *et al.*[18] are seeing exactly this collapse of the pseudogap. This, however, does not qualify their gap as a new gap (note that the reasoning is also valid if one takes the numbers from column two or five of Table I).

For an additional check on the arguments presented here, one can refer to the data listed in Table II. If one determines the superconducting energy, according to Fig. 1(b), as the pseudogap energy (measured in a one-electron experiment) at which the Fermi arc develops just above T_c, one gets from the data of Lee *et al.*[18] for their three samples (UD92, UD75, and OD86) and for two additional ones (UD80 and UD67) of

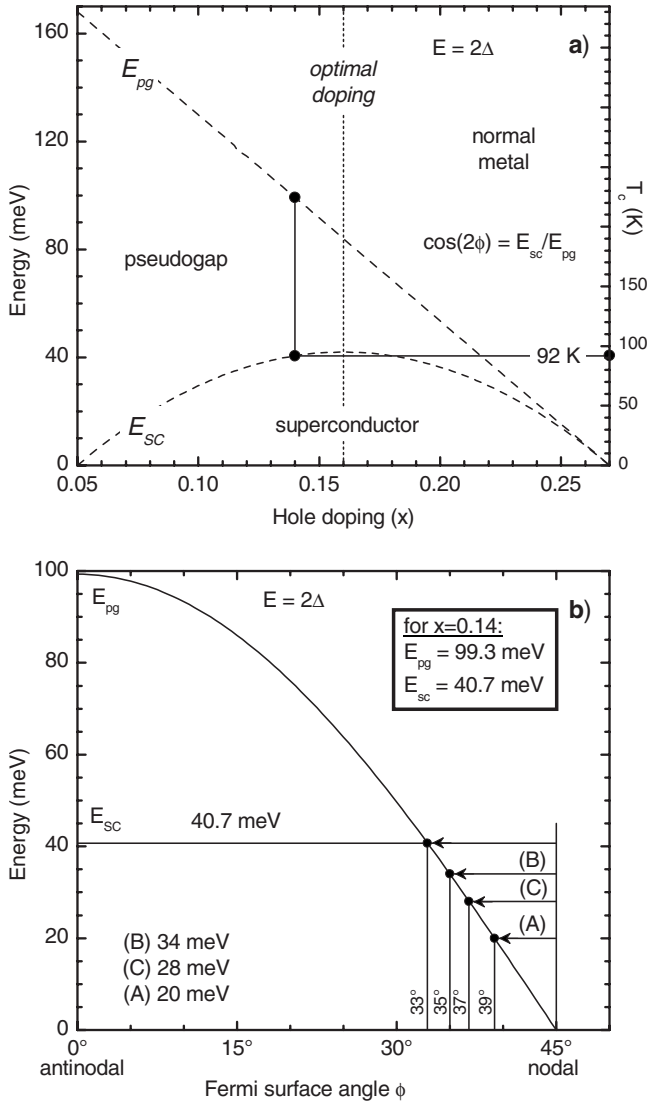

FIG. 2. Same as in Fig. 1; however, it was adopted to the experimental conditions of Ref. 18 for a slightly underdoped sample (UD92) with $x=0.14$.

Kanigel *et al.*[19] a ratio for $2\Delta/kT_c=5.4\pm0.4$. This is in agreement with the directly measured value of 5.2 ± 0.5.[7] Both studies[18,19] report the on data only for about 10 K above T_c, which leads to a slight enhancement of the Fermi-arc length relative to its value directly above T_c. Therefore, the gap may be overestimated by this method, which is reflected by the slightly larger ratio with respect to the directly measured one.

TABLE II. Superconductivity gap Δ_{sc} and T_c, taken for a number of Bi2212 samples from Refs. 18 and 19.

Δ_{sc} at the Fermi arc (in meV/in K)	T_c(K)	$2\Delta_{sc}/kT_c$
15 meV/180 K[a]	67	5.2
18 meV/216 K[a]	82	5.1
23 meV/276 K[b]	92	5.8
22 meV/264 K[b]	86	5.9
16 meV/192 K[b]	75	5.0
		5.4 average

[a]Reference 19.
[b]Reference 18.

In order to validate the arguments discussed here, some additional data from Refs. 18 and 19 are collected in Table III. In this table, the Fermi-arc angles (measured from the antinode) that are taken from the spectra are compared to those that are obtained by the method outlined in Fig. 1. In view of the apparent uncertainties involved in the procedure, the agreement between the different methods is gratifying. Therefore, the connection derived for the pseudogap and the superconducting energy in Figs. 1 and 2 is valid.

In addition, Table III contains the doping of the samples as determined by the commonly employed parabolic relation with T_c (Fig. 1). Finally, the length of the Fermi arc at T_c is given in degrees, as measured from $(\pi/2/\pi/2)$, which is $45°-\phi$ [in Table III, the indices (a)—(e) represent the data taken from Refs. 18 and 19 while the indices (f)—(h) represent the results as calculated from the general curves in Fig. 1(a)].

In order to check the internal consistency of the data, it was attempted to construct the doping dependence of the Fermi-arc length by the procedure indicated in Fig. 1, i.e., via the crossover of $E_{pg}\cos(2\phi)$ and $E_{sc}(\phi=0)$ for a particular doping x. This procedure results in the curve shown in Fig. 3 for the Fermi-arc angle ϕ (or the Fermi-arc length, namely, $45°-\phi$) as a function of the doping x. This curve has been obtained by using the straight line and the parabola in Fig. 1(a) which represents the averaged curves obtained by many methods for HTSC systems with a maximum T_c of 95 K and a maximum superconducting energy of 42 meV. Figure 3 also includes the data from Refs. 18 and 19. While the agreement between the simulation and the experiment is not impressive, the predicted trends are reproduced. This yields further support for the model on which the construction in Fig. 3 is based,: two gaps that both have a *d*-wave symmetry and the correlation of both gaps via the charge carrier density.

In Fig. 4, we finally present some data in support of the finding of Kanigel *et al.*[20] that the decay of the pseudogap is a thermally activated process. The data refer to the pseudogaps reported in Refs. 18 and 19 and the temperature (T^*) at which they disappear. This yields a straight line in Fig. 4, supporting the assumption that the decay of the pseudogap is a thermally activated process. The triangles are the antinodal pseudogaps and their pseudogap temperature for the UD80 and UD67 samples from Ref. 19. The circles are from the UD75, OD86, and UD92 samples from Ref. 18 for the Fermi-arc angles observed at 85, 93, and 102 K (all above T_c), respectively. The crosses are taken from Ref. 19 at Fermi-arc angles for the UD67 sample at 80 and 102 K, and for the UD80 sample at 90 K.

III. SUMMARY

A recently detected gap near the node by ARPES is not the superconducting gap (as has been stated) but the

TABLE III. Connection of the Fermi arcs with the pseudogap energy and the superconducting energy in Bi2212 samples

	UD92	UD75	OD86	UD80	UD67
ϕ [a]	27°	35°	25°	23°	35°
Doping x [b]	0.140	0.110	0.195	0.116	0.100
$E_{sc}/2$ [c](meV)	23	16	22	21	17
$E_{pg}/2$ [d](meV)	40	55	33	35	50
Fermi-arc angle ϕ [e]	27°	37°	24°	27°	35°
Fermi-arc length $45°-\phi$ [e]	18°	8°	21°	18°	10°
$E_{pg}/2$ [f](meV)	50	61	29	59	65
$E_{sc}/2$ [g](meV)	20	17	19	18	15
Fermi-arc angle ϕ [h]	33°	37°	25°	36°	38°
Fermi-arc length $45°-\phi$ [h]	12°	8°	20°	9°	7°
Reference	18	18	18	19	19

[a]From the Fermi-arc length in Refs. 18 and 19.
[b]From the experimental T_c via $T_c=95[1-82.6(x-0.16)^2]$ (in kelvins) in Fig. 1(a).
[c]From the experiment at Fermi-arc length.
[d]Experimental values at $\phi=0°$.
[e]From $\cos(2\phi)=E_{sc}/E_{pg}$.
[f]From the general curve in Fig. 1(a) $E_{pg}=168/0.22(0.27-x)$ in (meV) and the experimental T_c.
[g]From the experimental T_c via $kT_c=E_{sc}/5.1$.
[h]From the model $\cos(2\phi)=E_{sc}/E_{pg}$.

pseudogap. Yet, it follows the temperature dependence of the superconducting gap because, at the respective position in k space in the experimental conditions of Lee *et al.*,[18] it is smaller than the (maximum) superconducting gap. This lends further support to the two gap model of the HTSC.[8] In addition, it is demonstrated that the Fermi arc of a HTSC system at the angle ϕ can be calculated by setting equally the superconducting energy of a system and the term $E_{pg}\cos(2\phi)$ for the doping x of the sample.

We summarize the present understanding of the HTSC systems: The phase diagram in Fig. 1(a) shows that their pairing energy (pseudogap) is different from the superconducting energy (order parameter), where the latter one is given as the product of the pseudogap and the charge carrier

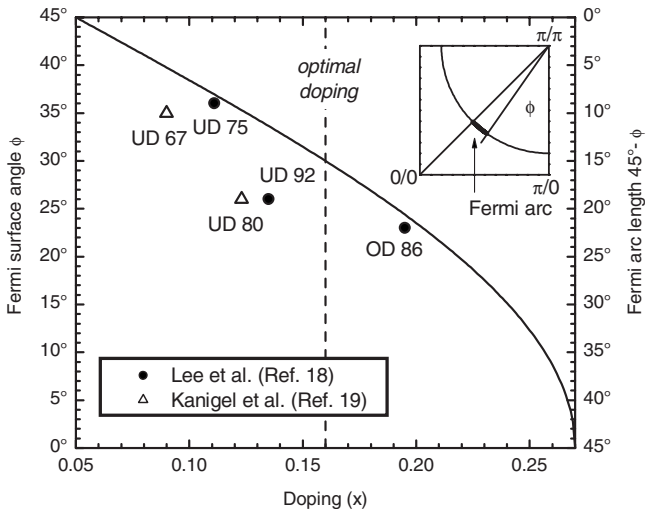

FIG. 3. Doping dependence of the Fermi-arc angle, as calculated from Fig. 1(b), for a HTSC sample with a maximum T_c of 95 K. The curve is obtained by setting equal the value of the superconducting energy $E_{sc}(x)$ for a particular doping x and the value of $E_{pg}(x)\cos(2\phi)$ for this sample, thus obtaining the angle ϕ, at which the Fermi arc occurs.

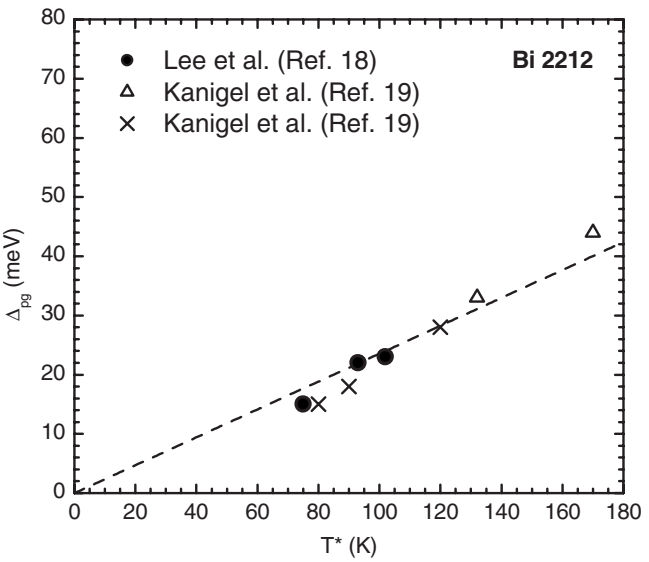

FIG. 4. Pseudogap energies ($\Delta_{pg}=E_{pg}/2$) and temperatures at which they disappear for a number of Bi2212 samples, from Refs. 18 and 19.

density. This characterizes the HTSC as Bose–Einstein systems;[12–14] however, near to the BCS region. Figure 1(b) shows that the two gaps have a $\cos(2\phi)$ behavior where ϕ is the angle with respect to the antinodal direction in the CuO_2 plaquette. From Figs. 1(a) and 1(b), it can be seen that in a temperature regime between T_c and T^* (T^* describing the temperature at which the pseudogap disappears), the Fermi arcs must occur for each doping between the nodal point and a ϕ value larger than $E_{sc}=E_{pg}\cos(2\phi)$. This is in accordance with the experimental results.

Considering all these observations, the HTSC can be described within the framework developed from the resonating valence bond concept.[9,10,17] This approach assumes that the superconducting state develops out of the insulating antiferromagnetic state. The doping of the antiferromagnetic state leads to singulets and their energy is measured by the pseudogap energy. The superconducting transition temperature is then given by the product of the pseudogap energy (decreasing linearly with increasing doping) and the charge carrier density (increasing linearly with doping) leading to the observed quadratic doping dependence of T_c.[9–11] In the regime, $T_c<T<T^*$ superconducting fluctuations occur as measured by the Nernst effect.[25]

ACKNOWLEDGMENTS

S.H. thanks the University of British Columbia in Vancouver for the hospitality extended to him during the academic year 2006–2007, where this research originated. At UBC, he profited very much from the intensive discussions with George Sawatzky and Andrea Damascelli. The work in Saarbrücken was supported by the Deutsche Forschungsgemeinchaft via SFB 277, TP B5.

[1] J. G. Bednorz and K. A. Müller, Z. Phys. B: Condens. Matter **64**, 189 (1986).
[2] T. Timusk and B. W. Statt, Rep. Prog. Phys. **62**, 61 (1999).
[3] A. Damascelli, Z. Hussain, and Z. X. Shen, Rev. Mod. Phys. **75**, 473 (2003).
[4] S. Hüfner, M. A. Hossain, A. Damascelli, and G. Sawatzky, Rep. Prog. Phys. **71**, 062501 (2008).
[5] S. Hüfner, M. A. Hossein, and F. Müller, Phys. Rev. B (to be published).
[6] M. Le Tacon, A. Sacuto, A. Georges, G. Kotliar, Y. Gallais, D. Colson, and A. Forget, Nat. Phys. **2**, 537 (2006).
[7] Y. Sidis, S. Pailhès, B. Keimer, P. Bourges, C. Ulrich, and L. P. Regnault, Phys. Status Solidi B **241**, 1204 (2004).
[8] M. R. Norman, D. Pines, and C. Kallin, Adv. Phys. **54**, 715 (2005).
[9] B. Eddeger, V. N. Muthukuman, and C. Gros, Adv. Phys. **56**, 927 (2007).
[10] A. Paramekanti, M. Randeria, and N. Trivedi, Phys. Rev. B **70**, 054504 (2004).
[11] V. J. Emery and S. A. Kivelson, Nature (London) **374**, 434 (1995).
[12] P. Nozieres and S. Schmidt-Rink, J. Low Temp. Phys. **59**, 195 (1985).
[13] Y. J. Uemura, Physica B (Amsterdam) **374-375**, 1 (2006).
[14] A. J. Leggett, *Quantum Condensates* (Oxford University Press, Oxford, 2006).
[15] O. Fischer, M. Kugler, I. Maggio-Aprile, and C. Berthod, Rev. Mod. Phys. **79**, 353 (2007).
[16] G. Deutscher, Rev. Mod. Phys. **77**, 109 (2005).
[17] P. W. Anderson, Science **235**, 1196 (1987).
[18] W. S. Lee, I. M. Vishik, K. Tanaka, D. H. Lu, T. Sasagawa, N. Nagaosa, T. P. Devereaux, Z. Hussain, and Z.-X. Shen, Nature (London) **450**, 81 (2007).
[19] A. Kanigel, U. Chatterjee, M. Randeria, M. R. Norman, S. Souma, M. Shi, Z. Z. Li, H. Raffy, and J. C. Campuzano, Phys. Rev. Lett. **99**, 157001 (2007).
[20] A. Kanigel, M. R. Norman, M. Randeria, U. Chatterjee, S. Suoma, A. Kaminski, H. M. Fretwell, S. Rozenkranz, M. Shi, T. Sato, T. Takahashi, Z. Z. Li, H. Raffy, K. Kadowaki, D. Hinks, L. Ozyuzer, and J. C. Campuzano, Nat. Phys. **2**, 447 (2006).
[21] F. C. Zhang and T. M. Rice, Phys. Rev. B **37**, 3759 (1988).
[22] H. Eskes, L. H. Tjeng, and G. A. Sawatzky, Phys. Rev. B **41**, 288 (1990).
[23] M. Eschrig, Adv. Phys. **55**, 47 (2006).
[24] J. Tranquada, *Handbook of High-Temperature Superconductivity* (Springer, New York, 2007), p. 257.
[25] Y. Wang, L. Li, and N. P. Ong, Phys. Rev. B **73**, 024510 (2006).